IET Radar, Sonar & Navigation

Research Article

IET Journals
The Institution of Engineering and Technology

Combining PRF staggering with phase-coded inter-pulse overlay to combat delay–Doppler ambiguities

ISSN 1751-8784
Received on 2nd April 2020
Revised 7th May 2020
Accepted on 27th May 2020
E-First on 15th July 2020
doi: 10.1049/iet-rsn.2020.0153
www.ietdl.org

Nadav Levanon[1] ✉

[1]*Department of Electrical Engineering – Systems, Tel Aviv University, 30 Chaim Levanon Street, Tel Aviv, Israel*

✉ *E-mail: levanon@tauex.tau.ac.il*

Abstract: Pulse repetition frequency (PRF) staggering is a well-established technique in the pulse-Doppler radar, used in order to increase the unambiguous range and Doppler and to minimise blind spots. The study offers a new staggering dimension that can increase the number of different staggering choices. The new approach is to add an inter-pulse coherent phase-coded overlay. The code is shorter than the number of pulses in each PRF batch and is repeated an integer number of times within the batch. A required property of the phase code is perfect periodic autocorrelation, namely zero autocorrelation sidelobes. In order to minimise the added complexity, the overlay codes use a two-phase or three-phase alphabet. As in a conventional PRF staggering, there are P coherent batches, each using a different PRF, with its matched phase-coded overlay. The performance analysis uses a conventional binary integration rule that declares detection if there were H, or more, individual detections in the P batches.

1 Introduction

Staggered pulse repetition frequency (PRF) [1, 2] is an important technique used in pulse-Doppler radar to mitigate range eclipsing and blind speeds. It can also serve as an electronic counter-countermeasure. Staggered PRF increases the unambiguous range and Doppler beyond what a single PRF provides. Within the beam dwell time, medium PRF radar usually cycles through several coherent processing intervals (CPIs), each using a different PRF. Staggered PRF processing usually performs additional incoherent binary integration of the CPI detections, using a decision rule of 'H, or more, detections in P CPIs'. The selection of PRFs and the binary integration parameters H and P are considered as an art in the radar design and are adapted to particular tasks.

This work proposes adding coherent, periodic, phase-coded overlays. Each CPI uses its unique overlay sequence and its unique PRF. In our example, all the CPIs have the same duration T_{CPI} and they all use the same number N of consecutive overlay repetitions. Thus, all the different overlays have identical duration $T_{\mathrm{C}} = T_{\mathrm{CPI}}/N$. We assume that the radar uses P different CPIs. The CPIs differ from each other by the number of pulses M_p within the overlay duration. Hence, a different PRF is given by $\mathrm{PRF}_p = M_p/T_{\mathrm{C}}$, $p = 1, 2, \ldots, P$. Therefore, the CPIs also differ in the number of elements in the overlay sequence, which must be equal to M_p. Fig. 1 displays pulse locations in two different overlays.

The reason for N repetitions of the relatively short overlay duration T_{C} is to reach a long CPI duration T_{CPI}. A long CPI provides a narrow Doppler resolution. The N consecutive repetitions of the phase-coded overlay are what imposes the crucial requirement that the phase-coded sequence must exhibit perfect periodic autocorrelation (PPAC). Section 2 lists several suitable sequence families. Section 3 outlines the structure of the waveform. The original pulses underneath the overlay can be any kind of identical compressed pulses. Our examples use linear frequency modulation (LFM) pulses with a time–bandwidth product of 20. The LFM pulse is generated by 50 identical frequency steps, each one of duration t_{b}. Hence, t_{b} is our basic time unit, to which all the time or delay axis are normalised.

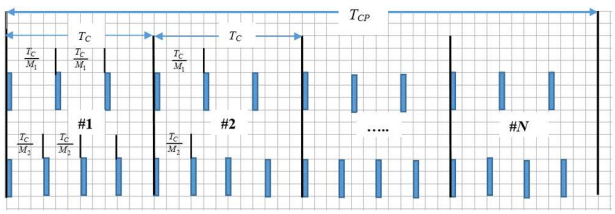

Fig. 1 *Pulse locations in two different overlays*

2 Sequences exhibiting PPAC

Suitable, rich and relatively simple overlay sequences can be found among Legendre and shift register sequences [3] and from few other small families.

Legendre sequences are available in all lengths that are odd primes. Odd primes can be divided into two families: (a) sequences of prime length M that also obeys $M = 4k - 1$, where k is a positive integer. Several short sequence lengths are {3,7,11,19, … }. Legendre codes based on those sequences can achieve PPAC if they use a two-phase, non-antipodal, alphabet. The two-code element values are $\{+1, \exp(\mathrm{j}\varphi)\}$. According to [4] the phase φ is given by

$$\phi = \cos^{-1}\left(-\frac{M-1}{M+1}\right) \tag{1}$$

(b) Sequences of prime length M, where M also obeys $M = 4k - 3$, e.g. {5,13,17,…}. Legendre codes based on those sequences can achieve PPAC if they use a three-phase alphabet [5, 6]. An anecdotal comment regarding the prime numbers of family (b): each one of them can be described by the sum of two squared integers. Some examples:

$$5 = 1^2 + 2^2,\ 13 = 2^2 + 3^2,\ 17 = 1^2 + 4^2$$

Expressions for the three phases used in legendre perfect codes, based on prime numbers of family (b), appear in rather cumbersome (22) and (23) of [6]. Rather than quote them, a simple and useful alternative is the MATLAB code in Section 8.1 of the Appendix.

More sparse than legendre sequences are shift register sequences, based on GF(2). They are available at lengths $M = 2^k - 1$. They use the same two-phase alphabet given in (1). Few short lengths are {3,7,15,…}. Shift register sequences

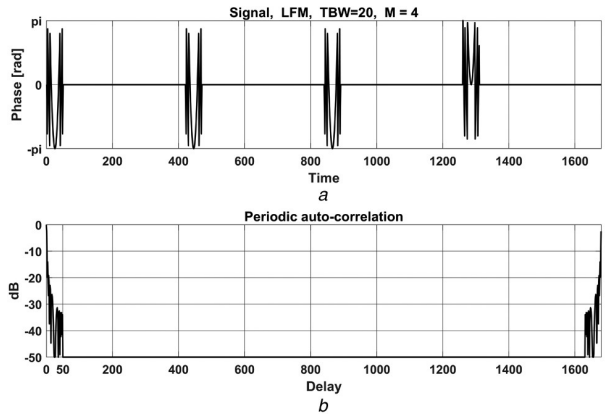

Fig. 2 *Barker 4 overlay on four LFM pulses*
(a) Phase evolution, ***(b)*** Periodic autocorrelation

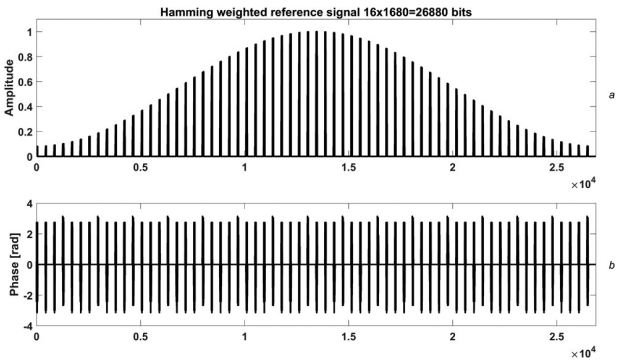

Fig. 3 *Reference signal with N = 16 code repetitions*
(a) Amplitude weighting, ***(b)*** Phase evolution autocorrelation

Table 1 Overlay parameters

Parameter	Symbol	Normalised value in Figs. 1 and 2
bit duration	t_b	—
pulse duration	t_p	$t_p/t_b = 50$
code duration	T_C	$T_C/t_b = 1680$
no. of pulses in T_C (= No. of code elements)	M	4
pulse repetition interval	PRI = T_C/M	1680/4 = 420
no. of code repetitions	N	16
CPI	CPI = $N \times T_C$	16 × 1680 = 26,880
no. of codes in binary integration	P	—
no. of required hits	H	—

generated using GF(3) are even more sparse. They are available at lengths $M = 3^k - 1$ and use a three-phase alphabet. The only short (<20) length is 8, and that sequence, given in [6], is $\{b\ b\ 1\ b-1-1\ 1-1\}$, $b = \exp(\mathrm{j}\,1.2309594)$.

One more sequence that exhibits PPAC is Barker 4, whose code is {1, 1, 1, −1}. Since we are dealing with periodic sequences, all the cyclic shifts of the listed sequences are suitable as overlays.

3 Overlay structure

The overlay structure is demonstrated with the help of Figs. 1–3 and Table 1. Fig. 2 displays one overlay code duration T_C containing $M = 4$ pulses. The top subplot displays the wrapped phase evolution of the four LFM pulses, which are parabolas. Barker 4 overlay changes the polarity of the fourth pulse. The polarity reversal, implemented by adding π radians, is clearly visible in the phase evolution of the fourth pulse. The bottom subplot displays the periodic autocorrelation of one code duration.

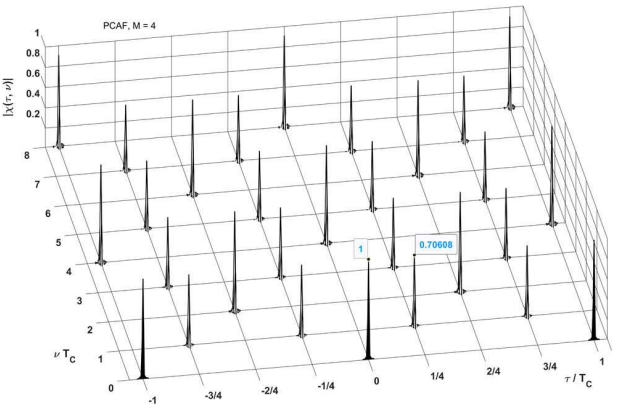

Fig. 4 *Partial PCAF of the 16 consecutive code periods*

This numerically generated display of the autocorrelation replaces an analytic analysis that would have required considerable space. The normalised dB scale, extending down to −50 dB, clearly shows zero delay sidelobes beyond the pulse duration of 50 bits, and extension of the unambiguous delay from one pulse repetition interval (PRI) to the code duration $T_C = M\,\mathrm{PRI} = 4\,\mathrm{PRI}$. As Table 1 indicates, the CPI contains $N = 16$ consecutive code periods. Recall that the CPI is defined in the receiver. In pulse-Doppler radar the number of pulses transmitted in a fixed PRF batch is larger than the number of pulses processed in the CPI ('filling pulses'), to accommodate targets and clutter at long range. Similarly, with the overlay, the transmitted signal has to contain at least one extra code period.

In order to reduce Doppler sidelobes the reference signal is amplitude weighted. Our example uses a Hamming window, as shown in the top subplot of Fig. 3. The transmitted pulses are not weighted.

The added overlay increased the unambiguous range by a factor of M, but changed the periodicity of the pulse train from the PRI to the code duration T_C. The resulted penalty is a decrease of the unambiguous Doppler by the same factor. This can be seen in the partial periodic cross-ambiguity function (PCAF) [7] of the signal, shown in Fig. 4. The term 'cross' enters because the amplitude weighting is used only on receive, hence the reference signal is not fully matched to the transmitted signal. Fig. 4 spans only the positive Doppler.

Each 'nail' in Fig. 4 represents a blind spot in the delay–Doppler response. Removing those nails is the task of the other CPIs and the binary integration that utilises all their individual detections to reach a final detection decision. Section 8.2 of the Appendix explains the locations and heights of the 'nails'.

4 Staggering CPIs with P different overlays

The PRF of each one of the P staggered CPIs is determined by the pre-set common code duration T_C and the number of elements in the code selected for that CPI.

In the given example $P = 4$ and the code lengths are $M = \{3,4,5,7\}$. The respective PRIs are: 560, 420, 336, 240 t_b.

As there is no common divisor to the four-code lengths, eclipsed ranges created by the transmitted pulses (and adjoining near clutter) in one CPIs do not coincide with eclipsed ranges in any of the other three CPIs. This result is demonstrated in Fig. 5.

The respective code sequences are:

$$M_1 \Rightarrow \{1,\ 1,\ b\},\ b = \exp(\mathrm{j}\,2.0944)$$
$$M_2 \Rightarrow \{1,\ 1,\ 1,\ -1\}$$
$$M_3 \Rightarrow \{b_1,\ b_2,\ 1,\ 1,\ b_2\},\ b_1 = \exp(\mathrm{j}\,1.2566),\ b_2 = \exp(\mathrm{j}\,2.5133)$$
$$M_4 \Rightarrow \{1,\ b,\ b,\ 1,\ b,\ 1,\ 1\},\ b = \exp(\mathrm{j}\,2.4189)$$

An important property of those four sequences is that their PAF 'nails' do not coincide. Instead of drawing three more PAFs, in addition to Fig. 4, we have plotted overhead views of all four PAFs

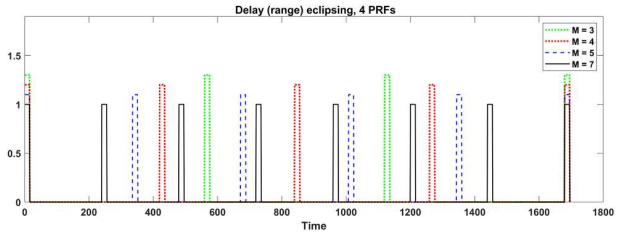

Fig. 5 *Eclipsed ranges by the four PRI*

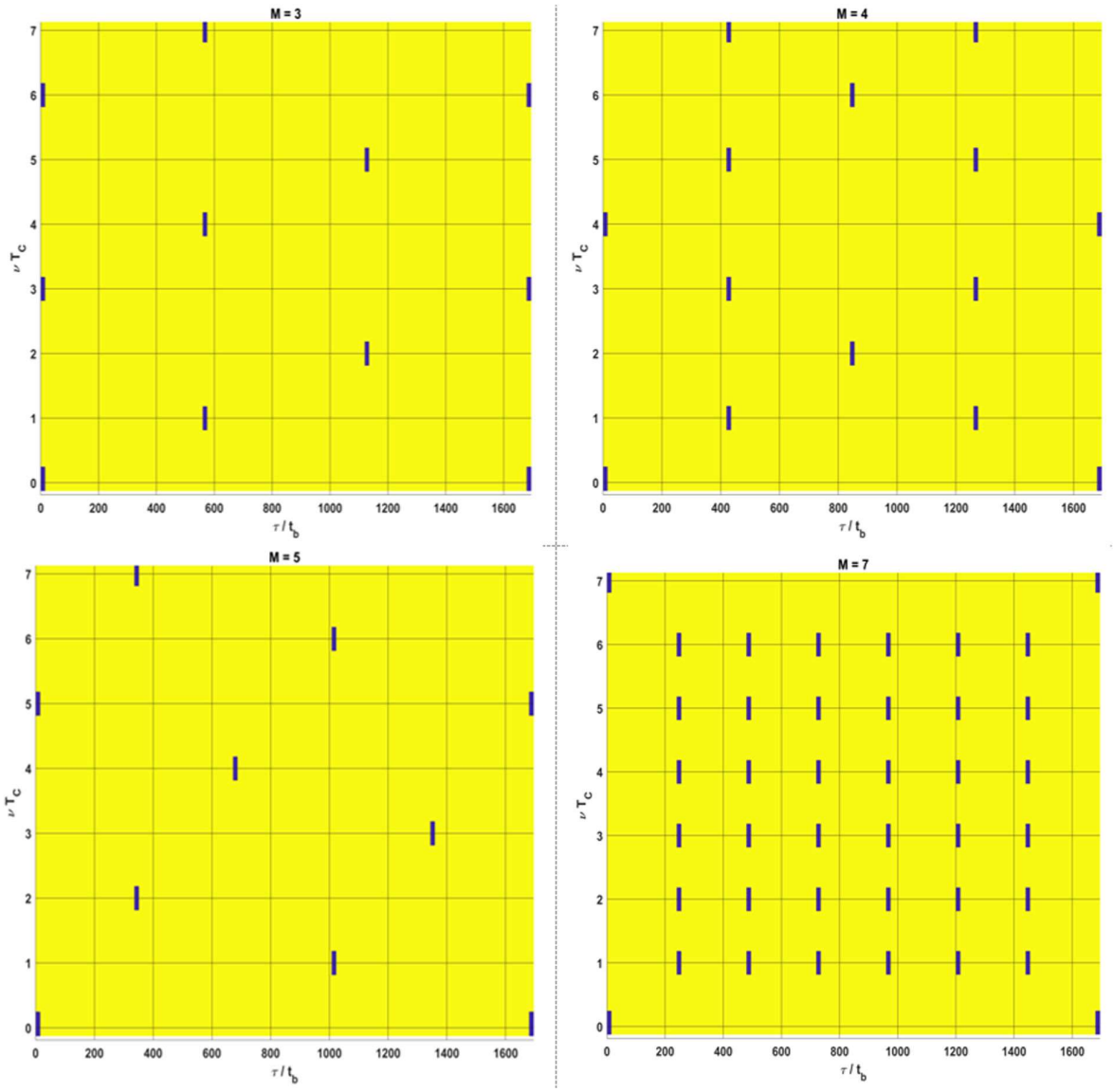

Fig. 6 *Ambiguity function blind spots (PAF peaks) of the four differently coded CPIs*

(Fig. 6). Only the first quadrants (positive delay and positive Doppler) are plotted. Each 'nail' is a blind spot because zero–Doppler clutter is folded into it.

Note from Fig. 6 that there are no blind spot coincidences. Namely, within the delay–Doppler area plotted in Fig. 6, a blind spot appears only once. Only the periodic main lobes, at zero Doppler and multiples of T_C, appear in all four PAFs. This important property is further demonstrated in Fig. 7, which displays the sum of the four plots in Fig. 6, with the correct height of each ambiguous 'nail'. The highest nails reach a value of one, but some are considerably lower.

Some recent publications [8, 9] suggest coherent integration of the differently staggered batches. We use the simple, conventional, non-coherent binary integration. Fig. 7 tells us what should be the binary integration rule ('H, or more, hits, out of P trials') required to reach a detection decision based on all P CPIs. Fig. 7 shows $2 \leq H$. This lower bound on H prevents detecting a ghost target in one of the Doppler blind spots, as well as on the range axis (zero Doppler). The upper bound on H is also obvious. Since at any delay–Doppler there could be a blind spot in only one of the P batches, allowing $H = P$ prevents a detection at such a cell. Therefore, the conclusion is $2 \leq H \leq P - 1$.

In our example $P = 4$, hence H can be 2 or 3. Which one is better? Beyond detection probabilities, address shortly, from the blind spots standpoint, a higher H raises the unambiguous Doppler.

Figs. 4 and 6 show that at $\tau = 0$, ambiguous Doppler peaks occur at

$$\nu_{\text{amb}} = k/(MT_C),\ k = 1, 2, \ldots \tag{2}$$

For such a peak to be detected as a ghost target it has to appear in H out of the P batches. In our example $P = 4$ and H can be 2 or 3. Since $M_1 < M_2 < M_3 < M_4$, the smallest ambiguous Doppler, for the two possible H values, is given in (3):

$$\begin{aligned} \min \nu_{\text{amb}}|_{H=2} &= M_1 M_2/T_C = 12/T_C \\ \min \nu_{\text{amb}}|_{H=3} &= M_1 M_2 M_3/T_C = 60/T_C \end{aligned} \tag{3}$$

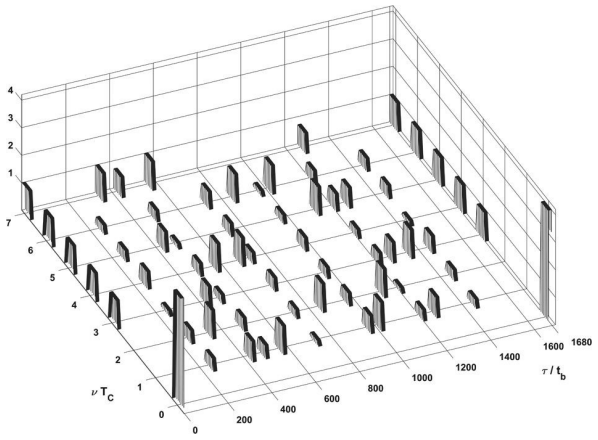

Fig. 7 *Sum of the four plots in Fig. 6*

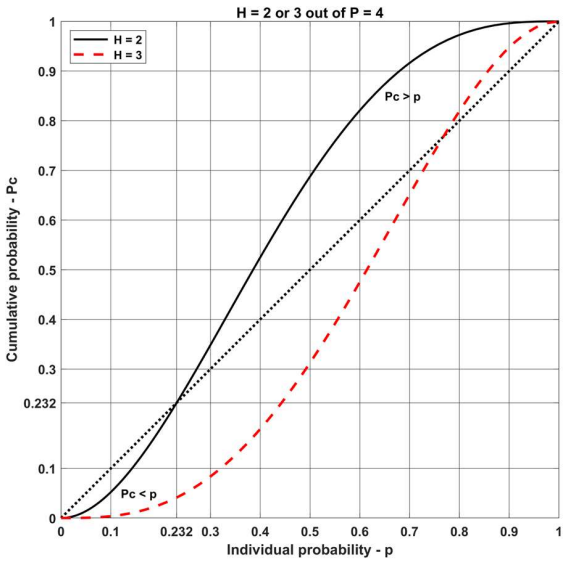

Fig. 8 *Binary integration detection performances*

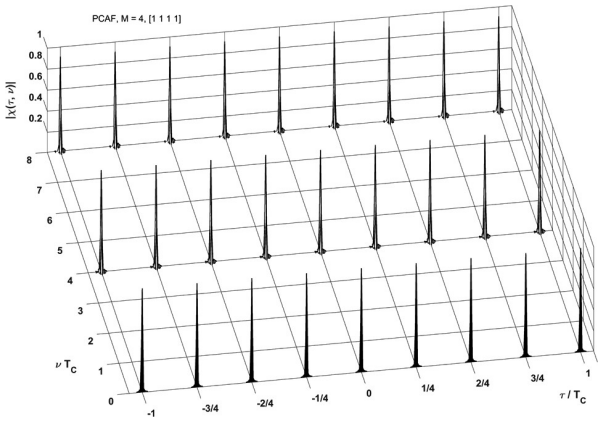

Fig. 9 *Partial PCAF of the 16 consecutive code periods with overlay [1 1 1 1]*

Thus, when seeking a clean blind speed map, the higher H should be preferred.

Another conclusion from (3) says that for the same T_C the ambiguous Doppler increases if larger M values are used. For example, in a system where $H = 3$, $P = 4$, $M_1 = 7$, $M_2 = 11$, $M_3 = 13$ and $M_4 = 15$, the smallest unambiguous Doppler occurs at $1001/T_C$.

It is important to note that in order to assure no coincidence of eclipsing, the code lengths M_i, $i = 1, 2, \ldots, P$, should not have a common devisor. For example 4 and 8 cannot be used together. The same for 5 and 15.

The above discussion recommended choosing $H = 3$ out of $P = 4$, rather than $H = 2$, in order to extend the unambiguous Doppler further. The detection performance of binary integration recommends the opposite. Fig. 8 considers the cumulative probability of detection P_c when binary integrating four individual detections, with equal individual detection probability p.

Fig. 8 shows that $H = 2$ improves the detection probability much more than $H = 3$. With $H = 2$, $P_c > p$ when $0.3 < p < 1$, which represents the span of detections, and $P_c < p$ when $0 < p < 0.2$, which represents the span of false alarms. With $H = 3$, $P_c < p$ when $p < 0.75$, which is undesirable.

5 Removing the phase-coded overlay

The contribution of the phase-coded overlay can be deduced by comparing it with a system that uses the same PRFs and coding duration T_C, but the overlays are all ones. For example, in Barker 4 case, whose PCAF appears in Fig. 4, we replaced the overlay of [1 1 1 −1] by [1 1 1 1]. The resulted PCAF appears in Fig. 9. Note that in Fig. 9 the 'nails' are of almost identical normalised height (≃1), while in Fig. 4 there is large height variability. One other prominent difference is the appearance of ambiguous 'nails' on the delay axis (zero-Doppler) at delay intervals of the PRI, where PRI = $T_C/4$.

The resulted sum of the four PCAF is given in Fig. 10, which should be compared with Fig. 7. Fig. 10 exhibits fewer blind spots but a large density on the zero–Doppler axis. In a bistatic radar, where the receiver is not eclipsed by the transmitted pulses and near-clutter, the role of ambiguous peaks on the zero–Doppler axis becomes more critical.

One possible benefit of the modified staggering is that it doubles the number of available staggering combinations with the same set of PRFs.

6 Conclusions

The paper uses existing knowledge from one radar field (periodic continuous wave signals) to enrich another radar field (PRF staggering in the pulse-Doppler radar). The result is a modification to classical PRF batch staggering of a coherent pulse train, by adding a different periodic coherent phase-coded overlay on each batch. Binary integration of the modified staggered batches produces extended unambiguous range and velocity, without blind spots.

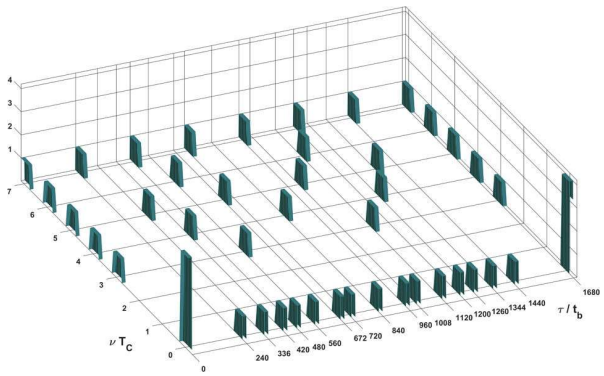

Fig. 10 *Sum of four blind-spot maps, no overlays*

The number P of differently overlaid batches needs to be three or more. Each batch contains N periodic phase-coded overlays. Each one of the P batches uses a different phase-coded overlay sequence with a different number of M_p of elements (pulses). There should be no common devisors between these numbers. All the overlays have the same time duration T_C. Hence, the PRI changes from batch to batch according to $\text{PRI}_p = T_C/M_p$. The final requirement is that each coherent code sequence must exhibit PPAC. 'Perfect' implies zero sidelobes.

The most suitable sequences that meet all those requirements are legendre sequences, with non-antipodal, two- or three-valued phase alphabet. Their length can be any odd prime number. The number of sequences can be supplemented by non-antipodal, two-valued, shift register sequences. Barker 4 is the only useful binary sequence.

The paper contains a design example of an overlay using the code lengths $M_1 = 3$, $M_2 = 4$, $M_3 = 5$ and $M_4 = 7$. The example is repeated for the same set of PRFs, but without the overlay.

7 References

[1] Alabaster, C.: '*Pulse Doppler radar, principles, technology and applications*' (SciTech, Edison, NJ, USA, 2012)

[2] Davis, P.G., Hughes, E.J.: 'Medium PRF set selection using evolutionary algorithms', *IEEE Trans. Aerosp. Electr. Syst.*, 2002, **38**, (3), pp. 933–939

[3] Golomb, S.W.: '*Shift register sequences*' (Aegean Park Press, Laguna Hills, CA, 1982, revised edn.)

[4] Golomb, S.W.: 'Two-valued sequences with perfect periodic autocorrelation', *IEEE Trans. Aerosp. Electr. Syst.*, 1992, **28**, (2), pp. 383–386

[5] Cohen, I., Elster, R., Levanon, N.: 'Good practical continuous waveform for active bistatic radar', *IET Radar Sonar Navig.*, 2016, **10**, (4), pp. 798–806

[6] Bomer, L., Antweiler, M.: 'Perfect three-level and three-phase sequences and arrays', *IEEE Trans. Commun.*, 1994, **42**, (2,3,4), pp. 767–772

[7] Levanon, N.: 'The periodic ambiguity function – its validity and value'. IEEE National Radar Conf., Washington, DC, USA, May 2010, pp. 1–7, DOI:10.1109/RADAR.2010.5494626

[8] Yin-Hu, Q., Wu, Y.J., Li, Y.C., *et al.*: 'Range-Doppler reconstruction for frequency agile and PRF-jittering radar', *IET Radar Sonar Navig.*, 2018, **12**, (3), pp. 348–352

[9] Tien, V.V., Hop, T.V., Nhu, N, *et al.*: 'A staggered PRF coherent integration for resolving range-Doppler ambiguitiy in pulse-Doppler radar'. The Int. Radar Symp., IRS 2019, Ulm, Germany, June 26–28

8 Appendix

8.1 Legendre sequences

MATLAB function for constructing a phase-coded periodic waveform of any odd-prime length, based on the legendre sequences (Fig. 11). The signal exhibits PPAC.

8.2 Delay response at normalised Doppler of $\nu T_C = 1$

Locations and heights of the peaks in the PCAF in Fig. 4. The discussion is based on the $M = 4$ case, and uses some MATLAB expressions.

Adding the overlay increased the signal's period from one PRI to $T_C = M$ PRI = 4 PRI. Hence, the Doppler peaks can appear only

```
function[s]=perfect_periodic_Legendre_waveform(M)
% Generates periodic coded signal using 2 or 3 phases
% The signal exhibits perfect periodic ACF
% M is any odd prime
Mspt=sprintf('%g element phase-coded waveform ',M);
if isprime(M)==0
   disp('Not a prime')
return
end
s=ones(1,M);
if rem((M+3)/4,1)==0
   c=0.25*(M-1);
   c1=2-1/c-1/(2*c^2);
   c2=1-1/c-1/(4*c^2);
   arg2=acos(-c1/2-sqrt((c1/2)^2-c2));
   s(mod((1:M-1).^2,M)+1)=exp(1i*arg2);
   s(1)=exp(1i*arg2/2);
else
   arg3=acos(-(M-1)/(M+1));
   s(mod((1:M-1).^2,M)+1)=exp(1i*arg3);
end
d=abs(ifft(fft(s).*conj(fft(s))));
figure, plot(d, 'k')
title(['Periodic ACF of ' Mspt ]);
end
```

Fig. 11 *MATLAB code for generating legendre signals*

at Doppler values that are multiples of $1/T_C$. This is why the dimensionless Doppler scale in Fig. 4 is normalised as νT_C. Correspondingly, the dimensionless delay is normalised as τ / T_C. The response on the delay axis is the absolute value of the periodic autocorrelation of the signal. The corresponding MATLAB expression is

$s = [1\ 1\ 1\ -1]$;
$M = \text{length}(s)$;
$X0 = 1/M$*abs(ifft(fft(s).*conj(fft(s)));
$X0 = 1\ 0\ 0\ 0$

When $\nu T_C = 1$, the Doppler-induced phase ramp accumulates 2π radians during the code duration. Namely, there is a change of $\pi/2$ between pulses. The response with the Doppler shifted signal becomes

dphi = 2*pi/M;
phi = dphi*[0:M−1];
sd = s.*exp(1i*phi);
$X1$ = 1/M*abs(ifft(fft(s).*conj(fft(sd))));
$X1 = 0\ 0.7071\ 0\ 0.7071$

That response is seen in Fig. 4, on the grid line of $\nu T_C = 1$. Repeating the run for the M_4 signal $\{1, b, b, 1, b, 1, 1\}$, where $b =$ exp(j 2.4189), yielded the response at $\nu T_C = 1$, as

$X1 = 0\ 0.4354\ 0.4489\ 0.1640\ 0.5991\ 0.3685\ 0.2955$